AAPS PharmSciTech (2019) 20: 157
DOI: 10.1208/s12249-019-1348-5

Research Article

Theme: Team Science and Education for Pharmaceuticals: the NIPTE Model
Guest Editors: Ajaz S. Hussain, Kenneth Morris, and Vadim J. Gurvich

Feedforward and Feedback Control of a Pharmaceutical Coating Process

Yuxiang Zhao,[1] James K. Drennen,[1,2] Shikhar Mohan,[1] Suyang Wu,[1] and Carl A. Anderson[1,2,3]

Received 20 December 2018; accepted 19 February 2019; published online 1 April 2019

Abstract. This work demonstrates the use of a combination of feedforward and feedback loops to control the controlled release coating of theophylline granules. Feedforward models are based on the size distribution of incoming granules and are used to set values for the airflow in the fluid bed processor and the target coat weight to be applied to the granules. The target coat weight of the granules is controlled by a feedback loop using NIR spectroscopy to monitor the progress of the process. By combining feedforward and feedback loops, significant variation in the size distributions and ambient conditions were accommodated in the fluid bed coating of the granules and a desired dissolution profile was achieved. The feedforward component of the control system was specifically tested by comparing the performance of the control system with and without this element by Monte Carlo simulation.

KEYWORDS: feedforward; feedback; process control; granule coating; near-infrared.

INTRODUCTION

Pharmaceutical manufacturing relies upon feedback controls to maintain the conditions necessary to manufacture quality products. Feedback loops are typically quite successful at maintaining prescribed conditions (1). However, standard feedback controls are susceptible to input disturbances and uncertainties (2). Thus, it is important that a control system be designed to accommodate foreseeable variation in the input to the process (3). Examples of typical disturbances in a pharmaceutical process include changes in raw material properties (4,5). Such disturbances can arise from chemical and physical properties of APIs and excipients. In response to such disturbances, feedback systems must wait until the disturbance has an observable effect on the control system, produce reduced quality product, or create an instability in the loop (6). In each of these scenarios, the quality of the product is at risk until the disturbance has been mitigated. Addition of a feedforward structure has the potential (7,8) to mitigate all of these risks to the quality of the product in a pharmaceutical manufacturing process.

Feedforward/feedback loops are used in this work in a control system for the application of a controlled release coating to granules in a fluid bed processing system. The granules contained theophylline as a model drug and the coating was a polyvinyl acetate-based coating (Kollicoat). Polyvinyl acetate forms pH-independent aqueous-insoluble film (9). The minimum film formation temperature was reported as 18°C without plasticizer and curing was found unnecessary (10,11). The intent of the coating was to modulate the dissolution of the API to match a twice-daily dosing regimen for theophylline (12). The ultimate goal of the coating process is to produce granules with a consistent release profile that meets appropriate specifications. Process models were created to predict the dissolution response based on the processing parameters.

A significant challenge in this process is the batch-to-batch variation in the sized distribution of the input material (granules). This has an impact on both the uncoated dissolution characteristics of the granules and the quantity of coating required (coat weight). As illustrated in Fig. 1, feedforward controls were built to account for the variability in the size distribution of the incoming granules and provide the coating process (and the feedback loops associated with it) set points that will convert a given batch of granules to a coated system that meets the required dissolution specifications. The specific set points from the feedforward loops are the fluidization air volume and the total quantity of coating to be applied. In essence, the feedforward loops establish set points for the process and the feedback loops achieve those set points. In this system, the feedback loops are inherently static, while the feedforward loop creates a dynamic response to changes in the input material. The feedback loop for controlling coat weight of the granules was based on a process analytical technology sensor. Near infrared spectroscopy

Guest Editors: Ajaz S. Hussain, Kenneth Morris, and Vadim J. Gurvich

[1] Duquesne University Graduate School of Pharmaceutical Sciences, Pittsburgh, Pennsylvania, USA.
[2] Duquesne University Center for Pharmaceutical Technology, 600 Forbes Ave, Pittsburgh, Pennsylvania 15282, USA.
[3] To whom correspondence should be addressed. (e–mail: andersonca@duq.edu)

(NIRS) was used to monitor the coating process and stop the process based on the required coat weight from the feedforward loop. The combination of feedforward and feedback loops created a control system that was capable of mitigating variation in the input materials and producing a product with consistent dissolution profiles.

This paper is organized as follows: in "Materials and Methods", statistically designed experiments are used to understand the change of dissolution output in response to the designed variability in coating material and process variables. A Weibull curve fitting function that simplifies the dissolution profiles into two dissolution parameters is presented. In "Results and Discussion", process modeling and the optimization strategy for the feedforward loop are demonstrated. The NIRS predictive model for the feedback loop is then described. Finally, a Monte Carlo simulation is applied to demonstrate the capability of the combined feedforward-feedback control system.

MATERIALS AND METHODS

Materials

The theophylline-loaded granules were obtained from Purdue University, West Lafayette, IN. The granules were composed of 60% theophylline anhydrous, 19.5% lactose monohydrate, 18.5% microcrystalline cellulose, and 2% hydroxypropyl methylcellulose. They were produced by high shear wet granulation using a 10-L capacity granulator (Diosna P/VAC 10-60, Osnabruck, Germany) and dried in the oven at 45°C for 48 h. Aqueous polyvinyl acetate polymer dispersions (Kollicoat SR 30D, Lot #: 57675147G0 and 58378447G0) were donated by BASF, Ludwigshafen, Germany. Triethyl citrate (TEC, 99% purity, Lot #: C09Y001), used as a hydrophilic plasticizer, was obtained from Alfa Aesar, Ward Hill, WA. Talc (USP Grade, Lot #: iEF0433), used as an anti-tacking agent, was obtained from Spectrum, New Brunswick, NJ. FD&C blue 1 lake (Lot#: A992), obtained from Warner Jenkison Company, St Louis, MO, was employed as a color marker to track the coating progress. All reagents utilized for assay and dissolution testing were HPLC grade.

Design of Experiments

This study focused on the development of a control system for fluid-bed coating of granules to control dissolution. A process model that predicts dissolution output from process and material variables is necessary, since it serves as the foundation of the control system. Two experimental designs (Fig. 2) were developed and conducted: (1) a full factorial design (calibration design) to gain process understanding and develop the process model and (2) a D-optimal design (test design) to test the process model. Full experimental designs are found in Appendix 1 and 2.

The calibration design included 10 coating runs using a three-factor full factorial design with two replicated center points. The center points were produced to determine pure error (random batch-to-batch variability) and check the non-linear effect. The factors were granule size distribution, relative humidity, and fluidization air volume. A fourth factor, target weight gain, was studied at three levels for each of the design points. The other process parameters, such as inlet air temperature, spray rate, atomization air pressure, and product temperature, were explored in preliminary studies and were kept constant in all experiments to prevent agglomeration of granules during coating. The levels of factors are shown in Table I. Five levels of granule size distributions were identified from the received granule batches. The lowest, medium, and highest levels of the five granule size distributions were included in the calibration design. The variability of relative humidity was caused by the change of seasons and thus the levels were ranges (20–30%, 40–50%, and 70–80% RH) instead of exact values. The seasonal dependence of relative humidity constrained the randomization of experiments in both calibration and test designs. Fluidization air volume was an experimentally controlled process parameter that was adjusted at two extreme and one center levels. The design levels of the three factors (granule size distribution, air volume, and relative humidity) are illustrated in Fig. 1, including both calibration and test sets. Target coating weight was the fourth factor and was varied by sampling granules after spaying for 80, 110, and 140 min. This target weight gain is expected to have a substantial impact on the quality attributes of the product as it is known to control dissolution of coated granules (13,14). The sample size was 10 g per time point. However, the weight gain cannot be accurately controlled without real-time monitoring due to variable polymer deposition efficiency. Therefore, NIR spectra were recorded during the coating process to facilitate the development of the NIRS-weight gain model. The calibration set included 30 design points in total (10 coating experiments × 3 sampling times = 30).

The test design included all five particle size levels of incoming granules. A total of nine coating runs were conducted using a D-optimal design (based only on granule size distribution, air volume, and relative humidity) to accommodate the limitation of granule supply. The D-efficiency was optimized using JMP software (Version 13, SAS institute, Cary, NC). Samples were taken at 85, 105, and 125 min after spraying for weight gain measurements and corresponding NIR spectra were recorded. The sample size remained as 10 g per time point. The sampling time points were adjusted to allow the weight gain of test samples being within the range of calibration samples. The test set included 27 design points in total (9 coating experiments × 3 sampling times = 27).

Granule Coating

The theophylline granules were coated in a minilab top-spray fluid bed processer (Diosna Dierks & Söhne GmbH, Osnabruck, Germany). The fluid bed processor was composed of a 3-l bowl with two sensors (a temperature sensor and a near infrared spectroscopic probe) and a 1-mm nozzle two-fluid spray gun. The coating suspension was supplied by a peristaltic pump. Atomization air pressure was manually controlled by adjusting the air gauge on the fluid bed. The fluidization air volume, inlet air temperature, and pump rotation speed were controlled by a DeltaV control system.

The coating dispersion (Table II) was prepared by diluting the aqueous polyvinyl acetate polymer dispersion with water. Triethyl citrate was added with continuous stirring of a magnetic stirrer. Talc and Blue Lake were then added and mixed for 6 h. Prior to coating, the dispersion was screened through a 180-μm screen.

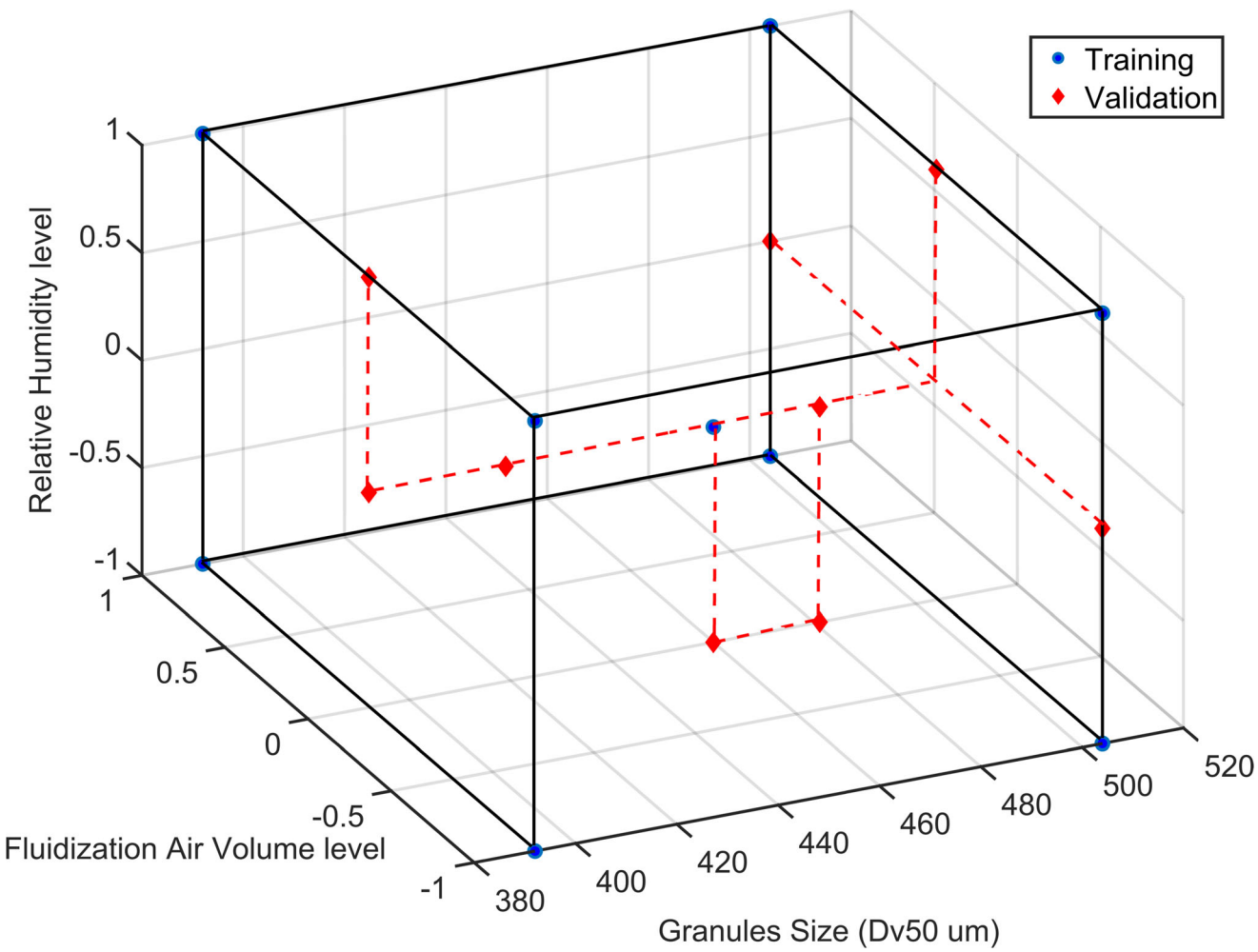

Fig. 1. The schematic of the control strategy. FFC: feedforward control, FBC: feedback control

The starting batch size of 400 g was selected for all coating experiments. The minilab fluid bed was preheated to 30°C before charging the granules. The spray started after the granules were equilibrated to the desired product temperature (33°C). Atomization air pressure (1.6 bar) and fluidization air volume (based on design points) were fixed while the inlet air temperature was adjusted during the spray rate ramp-up to maintain the desired product temperature. The spray pump speed ramped up from 2.5, 4, to 5.5 rpm (approximately 3, 4, and 5 g/min spray rate) in 10 min and then was kept constant at 5.5 rpm. Room temperature and ambient relative humidity (RH) were monitored for all individual batches. Samples were taken after spraying for 80, 110, and 140 min and stored in a desiccator at 35°C to allow the granules to be completely dried prior to dissolution test. The solid state of theophylline was examined by powder X-ray diffraction to ensure that no detectable levels of the hydrate form had been formed. The powder X-ray diffraction patterns of coated granules with presence/absence of theophylline monohydrate are shown in Appendix 3.

Test Methods

Granule Size Characterization

The granule size distributions of uncoated and coated granules were measured using a CANTY SolidSizer dynamic image analyzer (JM Canty, Inc., Buffalo, NY). The CANTY SolidSizer is a lab-scale image-based analyzer for dry particle size measurement. Granules were fed into a vibrating chute

Table I. Full Factorial Design-Design Levels

Variable name	Lowest level (−1)	Lower level (−0.5)	Center point (0)	Higher level (0.5)	Highest level (+1)
Granule size (Dv50, μm)	392	419	460	480	504
Ambient relative humidity (% RH)	20–30	–	40–50	–	70–80
Fluidization air volume (m^3/h)	25	–	30	–	35

Table II. Formulation of the Coating Dispersion

Component	Function	Concentration (*w*/*w* %)
Polyvinyl acetate polymer dispersion (PVAc)	Coating polymer	15
Triethyl Citrate (TEC)	Plasticizer	0.75
Talc	Anti-tacking agent	2.25
Blue Lake	Color agent	0.15
Deionized water	Solvent	81.85

and precisely released in front of a bright field. A high-resolution camera continuously collected images of free falling particles through a magnifying lens. The vibrating frequency of the chute was automatically adjusted by the instrument to maintain 10 particles on each image. The CANTY software analyzed the 2D images and output the granule size/shape information. Upon analyzing the images, a filter threshold was set to exclude the particles with aspect ratios larger than 2 to potentially eliminate overlapping particles. The circular equivalent diameter from the image analysis was used to describe the granule size.

Theophylline Assay, Loss on Drying and Percentage Weight Gain

The potencies of uncoated and coated granules were determined using a UV/Vis spectrometer (Agilent, Santa Clara, CA). To prepare the sample solution, 150 mg of uncoated granules was precisely weighed and dissolved in 500 mL DI water *via* 60-min sonication (Branson 8510 ultrasonic cleaner, Branson Ultrasonic Corporation, Danbury, CT). Three replicates of samples were prepared for every batch, and three repetitions were collected for each replicate. Reference cells that contained only DI water were collected each time the UV/Vis test started. The sample absorbance value at a single wavelength (272 nm) was recorded to predict API content by interpolating a five-point linear regression calibration model of theophylline content. The same method was applied to coated granules for API content with one additional step: the coated granules were ground prior to the dissolution and sonication.

Loss on drying measurement was performed using a moisture analyzer Computrac Max-2000 (Arizona Instrument LLC, Chandler, AZ). Approximately, 1 g of granules was ground using mortar and pestle. The ground powder was precisely weighed in the aluminum pan by the instrument prior to the test. The testing temperature ramped up from 35 to 110°C then stabilized at 110°C until the weight change of the powder was less than 0.01%. The percentage loss of the powder was recorded as loss on drying value (LOD). Percentage weight gain from coating is calculated based on the result of assay and loss on drying (LOD) from both coated and uncoated granules, as shown in Eq. 1.

$$\%weight\ gain = \frac{\frac{API\ content_{uncoated}}{(1-LOD_{uncoated})} - \frac{API\ content_{coated}}{(1-LOD_{coated})}}{\frac{API\ content_{coated}}{(1-LOD_{coated})}} \times 100 \quad (1)$$

Near Infrared Spectral Measurement

A NIR spectrometer (model: NIR-256-2, Control Development Inc., South Blend, IN) and halogen light source with a bifurcated fiber optic probe (Ocean Optics, Dunedin, FL) was used in this study to monitor the coating process, particularly for inline coating weight gain control. The probe was inserted into the fluid bed bowl in direct contact with the coated material. Each spectrum was acquired in real time by averaging 16 scans over the range of 1077–2226 nm with a resolution of 1 nm. The integration time for one scan was approximately 0.015 ms, varying by 0.002 ms for different batches. A near-infrared spectrum was recorded every 5 s, averaged from 16 spectra. The raw spectral data were processed using Matlab software (with Optimization Toolbox, version R2017a, the Mathworks Inc., Natick, MA) and PLS Toolbox (version 8.2.1) by Eigenvector Research (Manson, WA).

In Vitro Drug Release

The *in vitro* drug release studies were conducted on the encapsulated coated theophylline granules (400 mg coated granules per capsule) in 900 mL of DI water using a USP apparatus II–paddle type at 75 rpm and 37 ± 3°C. The capsules were dropped into the dissolution media using spiral capsule sinkers. The samples were drawn every 10 min using an auto sampler and measured using a UV/VIS spectrometer (Agilent 8453 UV-Visible Spectrophotometer G1103A, Agilent Technologies, Cranberry Twp, PA) at 272 nm wavelength. The fraction of drug released was normalized to 100% released; the time point at 1440 min used for that purpose. Three replicates were tested for each design point. The dissolution profiles were used as the responses for process modeling. A two-parameter Weibull function including a scale factor λ and a shape factor k was used to fit the dissolution curve as the following equation.

$$Fraction\ of\ drug\ released = 1 - e^{-\left(\frac{t}{\lambda}\right)^k} \quad (2)$$

RESULTS AND DISCUSSION

This study provides a demonstration of a process modeling-based control system coupled with real-time monitoring tools. The control system (Fig. 1) consists of feedforward and feedback loops to ensure the consistency of product dissolution profiles. The terms “feedforward” and

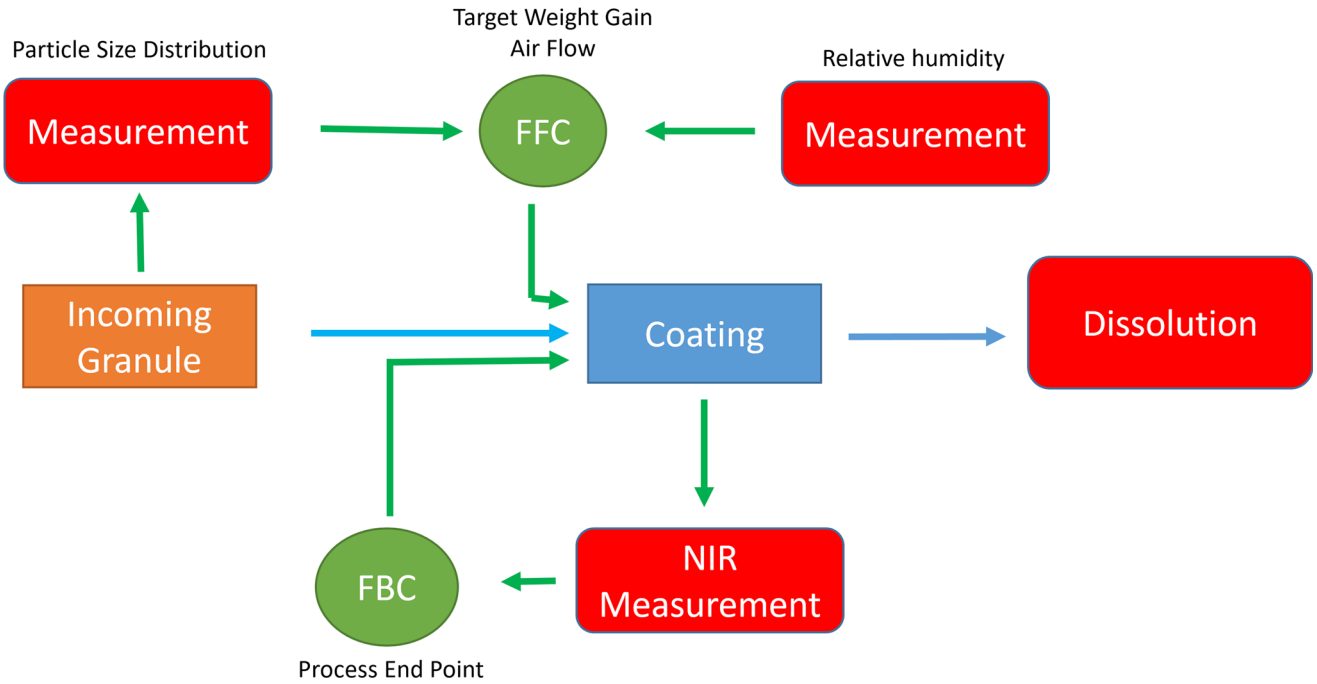

Fig. 2. Illustration of the design of experiments including both calibration and test sets

"feedback" were used in a generalized manner. The feedforward control employed a process model to predict the desired fluidization air volume and target weight gain based on incoming granule size distribution and relative humidity prior to the coating operation. The feedback control monitored weight gain using a NIRS predictive model and terminated the coating process when the target was achieved.

Dissolution Results and Curve Fitting

The raw dissolution profiles from both calibration and test sets are presented in Fig. 3a. The calibration design covers a broad range of dissolution profiles and the test data falls within the designed range. The dissolution profiles were compressed from 60 data points (time points) to two dissolution parameters from a best fit of a Weibull function to the data. An unconstrained non-linear fitting method was applied using Matlab 2017a and optimization Toolbox. Curve fitting of the Weibull function gave high R^2 values (0.975–0.998) for all dissolution profiles, indicating that the variance in the dissolution profiles was captured by the Weibull function-based models. The residual profiles of the fit were examined, revealing a pattern (Fig. 3b) that indicated the fitting caused bias between the measured and fitted data. The measured fractions of drug released were consistently lower than the fitted data during the initial 30 min. The residual

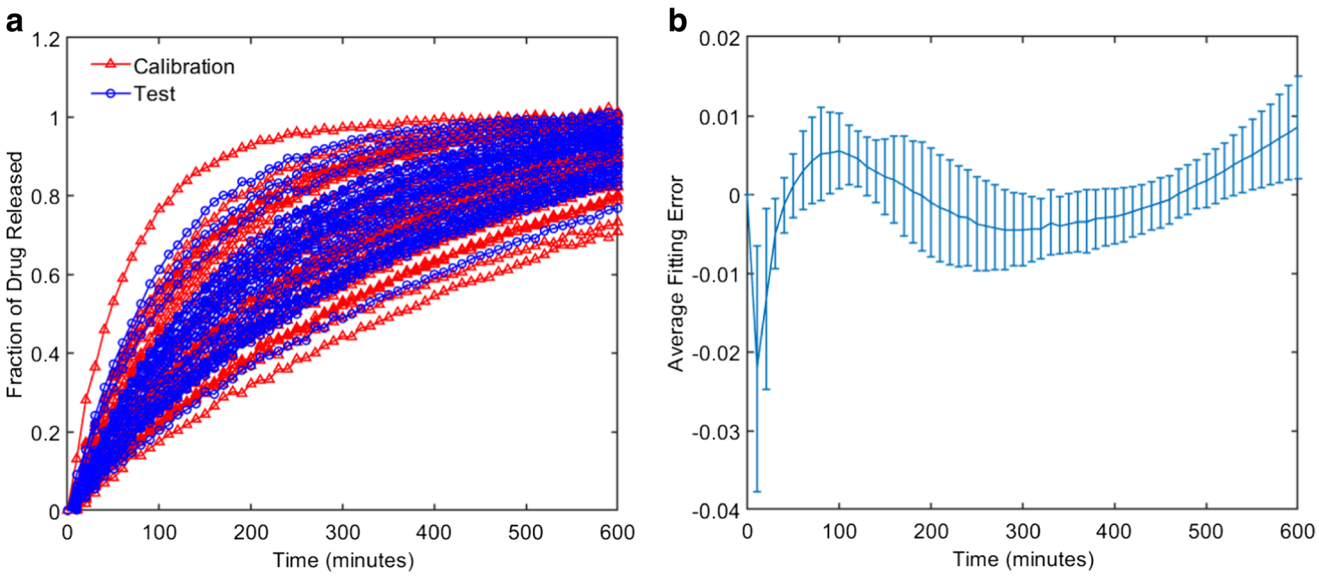

Fig. 3. **a** Measured dissolution profiles of calibration and test designs; **b** average error and the standard deviation of the average error from Weibull function curve fitting

pattern from 30 to 600 min was a continuous smooth wave shape. The error bars indicate that the pure error was significantly larger than the bias at most of the time points (the confidence intervals included zero). The bias and pure error were utilized for the evaluation of model performance and control analysis in the Monte Carlo simulation.

Feedforward Control: Process Model

Process models were established by regressing dissolution parameters, scale factor λ and shape factor k, on four types of predictors: (1) fluidization air volume, (2) weight gain, (3) particle size distribution, and (4) relative humidity. Fluidization air volume and weight gain were continuous variables. Particle size distribution was given in the form of a probability density function, which included 9 variables as the probabilities of a particle being in 9 size intervals: 50–150, 150–250, 250–350, 350–450, 450–550, 550–650, 650–750, 750–850, and 850–950 μm. However, there were only three levels of particle size distributions in the calibration design. The 9 variables of the three levels were decompressed into two latent variables (PC1 and PC2) using principal component analysis (mean centering of PCA reduced one dimension of the dataset). The first latent variable explained 87.7% variance of the particle size distribution and the second latent variable explained the remaining 12.3% variance. The two latent variables (in place of the nine density probability values) were used as predictors in the regression. Relative humidity was treated as a nominal variable. Two dummy variables were coded to represent the three levels of relative humidity.

Partial least squares regression (PLS) was employed to execute the regressions for the calibration set. The models were optimized using a cross-validation method of random-subset with five data splits and five iterations, randomly partitioning the full calibration into five equal-sized subsets. Of the five subsets, one was retained as validation data for model testing and the remaining four were used as calibration data. For one iteration, five results were generated from the five subsets and were averaged to produce a single root means squared error of cross-validation (RMSECV). Five iterations were applied and the RMSECVs were averaged. The objective of latent variable selection is to minimize simultaneously the number of latent variables and cross-validation error, shown in Fig. 4c, d. For both scale and shape factor models, three latent variables were selected. The fact that both RMSECVs and RMSEPs reached their plateaus after three latent variables suggested that the model was not over-fitting the data. The number of chemical and physical factors is far greater than the three latent variables used to model the data, further suggesting that the number of selected latent variables does not put the model at risk for over-fitting. The test set data was projected onto the process models. The coefficient of determination and root mean squared errors of prediction (RMSEP) were calculated to evaluate the model performance on the independent test data. The process model was mathematically expressed as the following equations:

for scale factor λ,

$$\lambda = 0.22 \times X_1 - 4.88 \times X_2 - 4.79 \times X_3 - 7.61 \times X_4 - 0.18 \times X_5 + 21.21 \times X_6 - 171.4 \quad (3)$$

and for shape factor k,

$$k = -0.041 \times X_1 - 0.012 \times X_2 - 0.010 \times X_3 - 0.0015 \times X_4 - 0.012 \times X_5 + 0.0028 \times X_6 + 0.9350 \quad (4)$$

where X_1 = fluidization air volume; X_2=dummy variable 1 of relative humidity; X_3= dummy variable 2 of relative humidity; X_4= scores on PC1 of granule size distribution; X_5= scores on PC2 of granule size distribution; X_6= weight gain.

The predictors showed a strong correlation with the scale factor λ, with R^2 being 0.975 for calibration and 0.955 for cross-validation (Fig. 4a). It revealed that the model explained most of the dissolution variance in the designed space. The RMSEC and RMSECV were 16.1 and 21.6 (unitless). They are close to each other, indicating a lack of overfitting. The R^2 was 0.887 for the test set and RMSEP was 27.6. Both were lower than those of calibration and cross-validation, but they were still within an acceptable range, indicating that the model was robust against unknown disturbances that existed in the test set. Figure 4b depicts the correlation between the predictors and the shape factor k. The R^2 value was 0.816 for calibration, 0.736 for cross-validation, and 0.497 for prediction. The RMSEC, RMSECV, and RMSEP were 0.0221, 0.0265, and 0.0259. Although the prediction was not as accurate as the scale factor model, the model reduced the error significantly (F-test, $P < 0.05$) from the standard deviations of k values in calibration (0.0515) and test set (0.0349). The predicted scale and shape factors were utilized to reconstruct the dissolution profiles in the form of fraction of drug released (based on Eq. 2) at specific time points for calibration, cross-validation, and test, respectively. The RMSEC, RMSECV, and RMSEP profiles along the time points were calculated by subtracting reconstructed dissolution profiles from the measured dissolution profiles. The plot (Fig. 4c) showed that the error gradually increased from the time point 0 to 100 min in all three profiles. From the time point 100 to 250 min, the error remained above 0.025 for RMSEC, 0.03 for RMSECV, and 0.035 for RMSEP. After the time point 250 min, all three error profiles showed a decreasing trend over time. It was consistent with the raw dissolution profiles (Fig. 3a) where significant variability was observed from second hour to the fourth hour between the design points. Given that all error profiles were below the threshold of 5%, the model performance was considered acceptable for the purpose of feedforward control.

A constrained global searching algorithm (15,16) coded in Matlab and the Optimization Toolbox was utilized in the application of the process model as a control system. The algorithm searched for the solution of process parameters, fluidization air volume, and weight gain that minimized the cost function based on given granule size distribution and relative humidity. The cost function J was an expression of the difference between predicted and target dissolution parameters, shown as Eq. 5.

$$J = \left(\hat{\lambda} - \lambda_{target}\right)^2 + \left(\hat{k} - k_{target}\right)^2 \quad (5)$$

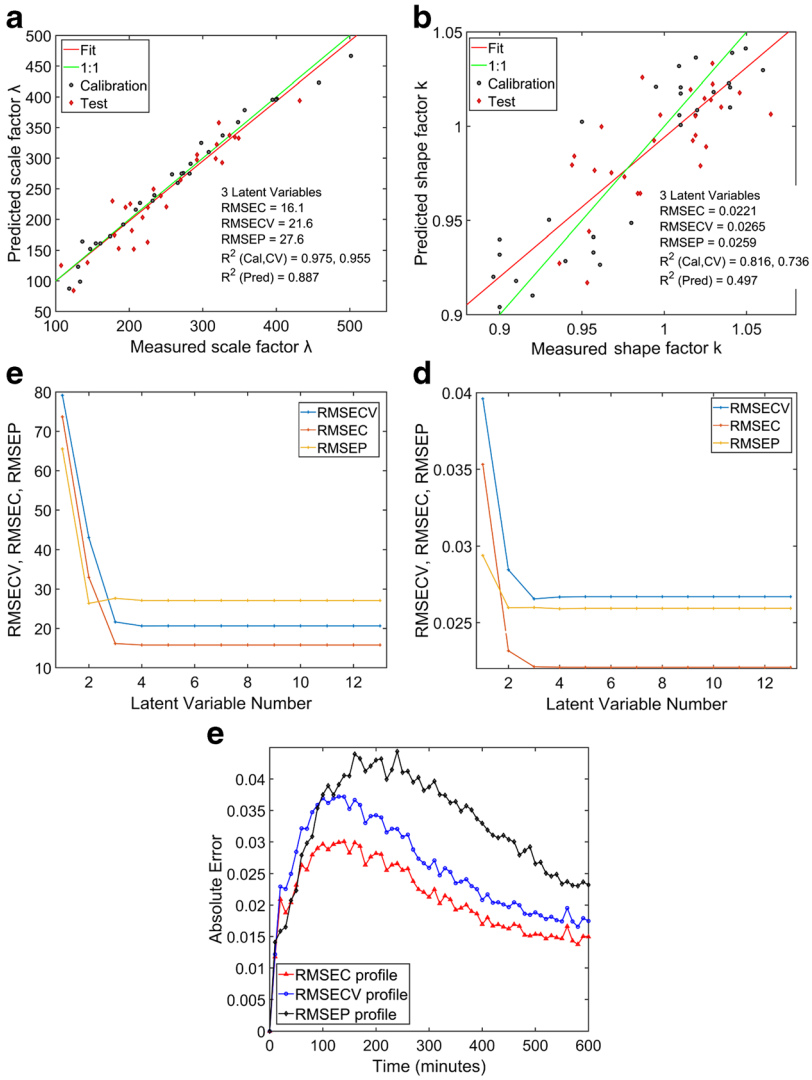

Fig. 4. The model performance of the dissolution prediction. **a** Predicted *vs* measured scale factor λ; **b** predicted *vs* measured shape factor k; **c** scree plot of the scale factor λ model: error *vs* number of latent variables; **d** scree plot of the shape factor k model: error *vs* number of latent variables; **e** absolute error *vs* time plot for the process model in terms of calibration, cross validation and prediction

where $\hat{\lambda}$ and λ_{target} were the model predicted and target scale factors; $\hat{k}$ and k_{target} were the predicted and target shape factors. The constraints were applied to limit the solved process parameters being within the tested range of the model: 25–35 m^3/h for fluidization air volume and 12–26% for weight gain.

Feedback Control: NIRS Model

The feedforward control provided the set-point of air volume and target weight gain for each batch while the feedback control used an NIRS predictive model to monitor the weight gain in real time and determined the process end. The NIRS model was calibrated using the 30 samples from the calibration design and validated on the 27 samples from the test design. The weight gain values of all samples were calculated from Eq. 1. Ten spectra of each design point were collected around the time point when the granule samples were drawn (from 25 s before to 25 s after the sampling). The spectral regions of 1077–1150 nm and 2100–2226 nm were noisy and thus excluded from the model.

The NIRS predictive model was developed using partial least squares (PLS). Since the main interference in the raw spectra (Fig. 5a) was the baseline shift, several preprocessing methods were evaluated to determine the optimum method. The number of latent variables was chosen along with the selection of preprocessing method. The cross-validation method used random subsets with 5 data splits and 5 iterations. It was found that a model with four latent variables (Fig. 5b) yielded the best results. The model included preprocessing of standard normal variate (SNV) followed by mean centering for spectral data and auto-scaling for weight gain data to provide the following calibration and prediction statistics (all values are absolute error): RMSEC of 0.003, RMSECV of 0.003, and RMSEP of 0.005 (Fig. 5c). The reduced Q residuals *vs* Hoteling T^2 plot (Fig. 5d) indicated that the most points of the test set fell in the 95% confidence

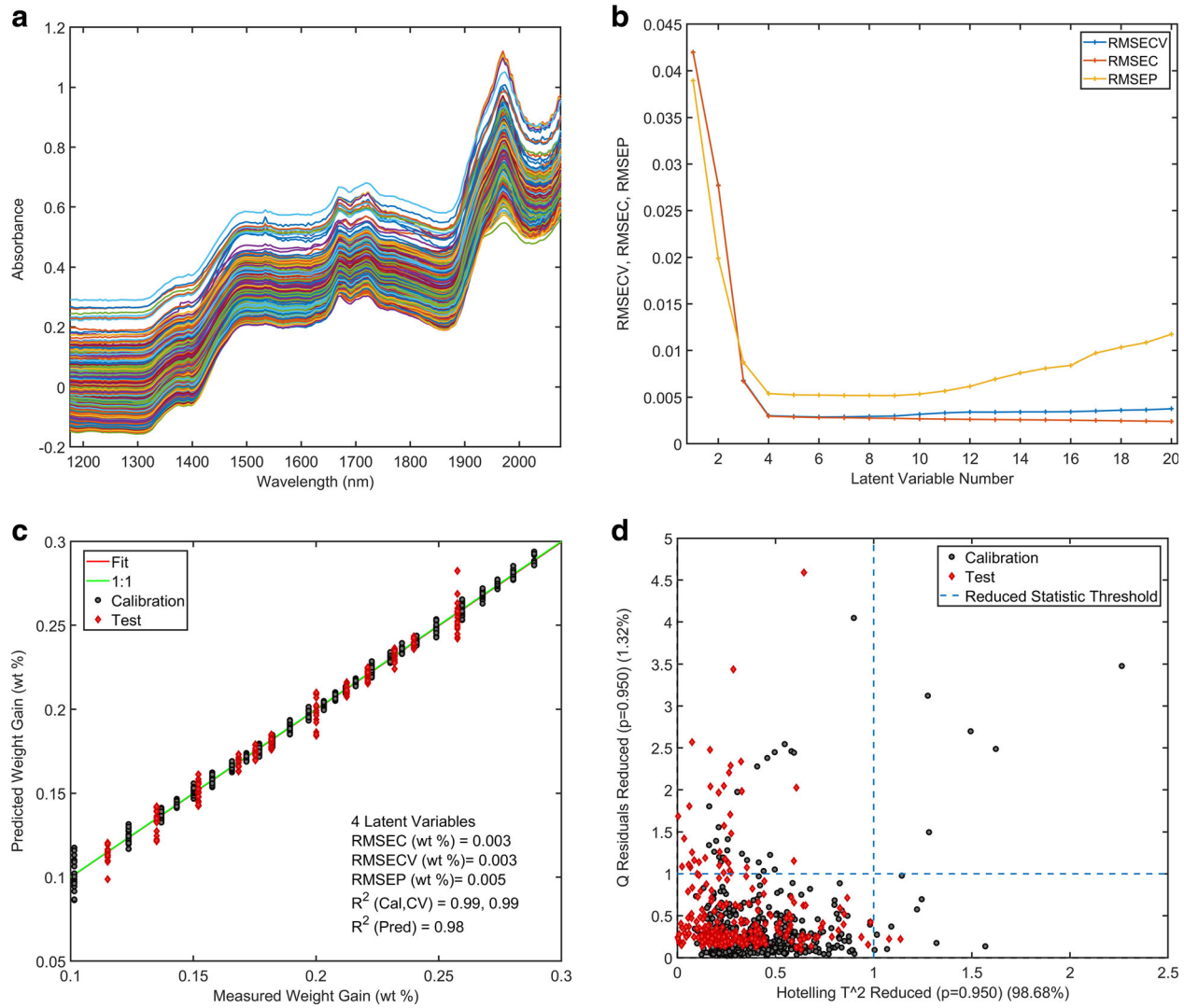

Fig. 5. NIRS predictive model: **a** raw NIR spectra of the calibration set; **b** scree plot for the optimized preprocessing method: SNV + mean centering; **c** predicted *vs* measured weight gain; **d** Q residual *vs* Hotelling T^2 plot

interval of the calibration, suggesting that they were not significantly different from the calibration data. The model utilized 99.68% variance of the spectral data to explain over 99% variance in weight gain for calibration. The total calibration range was from 0.10 to 0.29 fraction weight gain; the R^2 was 0.98 and an error of 0.005 (absolute) for the test set was observed.

Control Performance Analysis

The variability of the models introduced uncertainty to the control system. The variability arose from dissolution curve fitting, the NIRS model, and the process model. A mathematic expression of the dissolution profiles, with error terms, is described in Eq. 6

$$\textit{Fraction of drug released} = 1 - e^{-\left(\frac{t}{\lambda+\sigma(NIRS)+\sigma(\lambda)}\right)^{(k+\sigma(NIRS)+\sigma k)}} + \text{bias} + \text{pure error} \quad (6)$$

where $\sigma(NIRS)$ is from the error of weight gain from the NIRS model, (λ) and $\sigma(k)$ are the errors of dissolution parameters from the process models, bias and pure error are from the curve fitting method.

The capability of the controlled process was evaluated using a Monte Carlo simulation. Fifteen different initial conditions (5 levels of granule size distributions × 3 levels of relative humidity) were input to the simulation. An in-house dissolution specification (shown in Fig. 6a) including four intervals of percentage drug dissolved at specified time points (60, 120, 240, and 480 min) was employed to set a target for the control system. The center points of the intervals (20%, 37.5%, 67.5%, and 90%) were used as the dependent variable and the time points as the independent variable for fitting using the Weibull function. The scale and shape factors were subjected to the searching algorithm of feedforward control to generate target fluidization air volume and weight gain for each initial conditions. The distributions of pure error from curve fitting, the process models, and the NIRS model were all assumed Gaussian shape. The simulation algorithm ran in the following sequence: (1) one error value was randomly

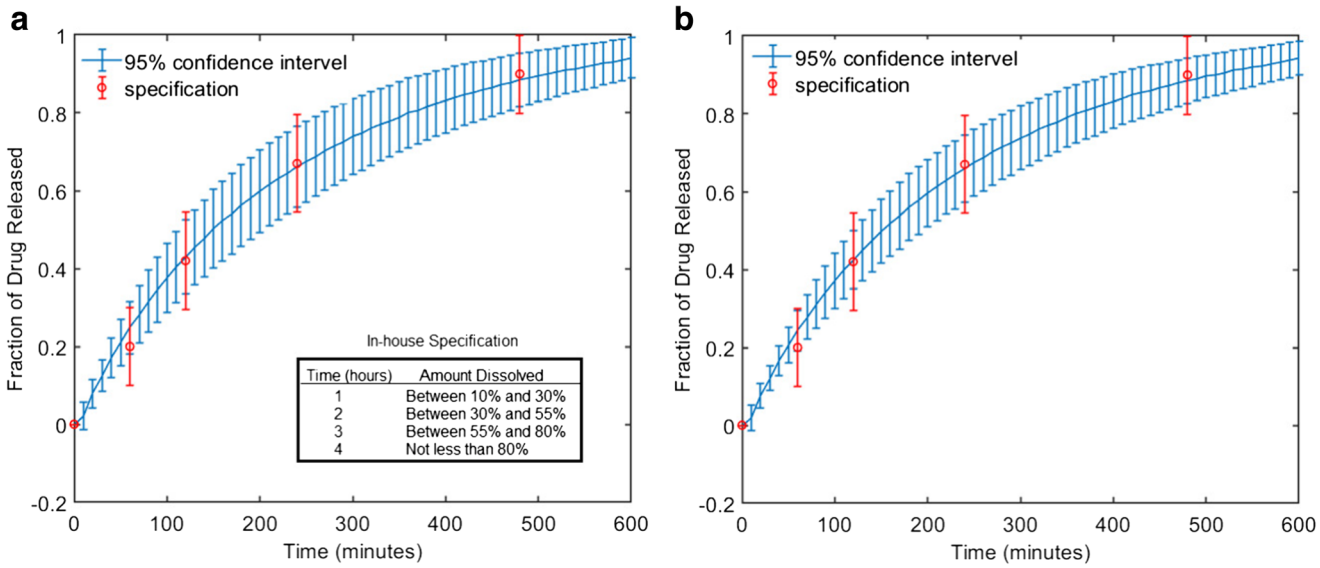

Fig. 6. Monte Carlo simulated dissolution profiles and 95% tolerance intervals for both **a** feedback control only and **b** combined feedforward-feedback control scenarios

selected from the error distribution of the NIRS model ($\sigma(NIRS)$) and applied to the target weight gain; (2) the error incorporated weight gain value was employed for the calculation of the scale and shape factors using the process models; (3) error values were randomly chosen from the error distribution of process models ($\sigma(\lambda)$ and $\sigma(k)$) and applied to the scale and shape factors, respectively; (4) the dissolution curve was reconstructed using the error incorporated scale and shape factors; (5) bias and a randomly selected pure error profile were applied to the dissolution curve to complete one loop of the simulation. The algorithm was repeated until the out of specification rate converged (10,000 times in this study) for each initial condition. In total, 150,000 dissolution profiles were generated and the 95% tolerance intervals were calculated for every time point from 10 to 600 min. In order to understand the contribution of the feedforward component of the control system, the same simulation algorithm was applied with and without feedforward component. The same initial conditions were used; however, the means of the 15 individual fluidization air volumes and weight gains were used to generate the scale and shape factors for the system without feedforward component. The 95% tolerance intervals across time points were calculated from the same amount (150,000) of dissolution profiles as the previous simulation.

The simulated dissolution profiles were compared to the in-house specification. The results showed that a coating batch had an 8.1% chance of failing to meet the dissolution specification without feedforward control. The failure rate decreased to 3.8% when the combined feedforward-feedback control system was applied. Figure 6 depicts that the 95% tolerance intervals of the combined feedforward-feedback system (Fig. 6b) were narrower than the system with only feedback control (Fig. 6a) for most of the time points. Compared to the other time points, the samples simulated without feedforward control tended to release fast and failed to comply with the specification in the early stage of dissolution (the specification interval at 60 min did not fully cover the 95% tolerance interval of the simulated dissolution profiles). The results suggest that intentional changes to the in-process parameters have the potential to mitigate batch-to-batch variation in the input if a well-designed feedforward loop is used.

CONCLUSION

The coating of granules in a fluid bed process using feedforward and feedback loops was studied. A combined feedforward-feedback control system was established based on process understanding and a comparison of the system with and without the feedforward component was evaluated using Monte Carlo simulation. The feedforward control adjusted the fluidization air volume and coating weight gain to mitigate the undesired impact of variable granule size and ambient relative humidity. The feedback control model utilized inline NIR spectroscopic monitoring to ensure that the target coat weight gain was achieved. The control strategy allowed for the fulfillment of process development stated in ICH Q8 "… the control of the process such that the variability (*e.g.*, of raw materials) can be compensated for in an adaptable manner to deliver consistent product quality. (17)"

ACKNOWLEDGEMENTS

We would like to thank Dr. Carl Wassgren and Dr. Dhananjay A Pai from Purdue University for the production of the theophylline granules.

FUNDING INFORMATION

The National Institute for Pharmaceutical Technology and Education (NIPTE) and the U.S. Food and Drug Administration (FDA) provided funds for this research. This study was funded by the FDA Grant to NIPTE titled "The Critical Path Manufacturing Sector Research Initiative (U01)"; Grant# 5U01FD004275.

APPENDIX 1 DOE TABLE FOR THE CALIBRATION DESIGN

Order of run	Granule size (Dv50, μm)	Fluidization air volume*	Relative humidity*
1	392 (level − 1)	1	1
7	392 (level − 1)	1	− 1
2	392 (level − 1)	− 1	1
8	392 (level − 1)	− 1	− 1
3	504 (level 1)	1	1
9	504 (level 1)	1	− 1
4	504 (level 1)	− 1	1
10	504 (level 1)	− 1	− 1
5	460 (level 0)	0	0
6	460 (level 0)	0	0

APPENDIX 2 DOE TABLE FOR THE TEST DESIGN

Order of run	Particle size (Dv50, μm)	Fluidization air volume*	Relative humidity*
1	460 (level 0)	0	− 1
8	392 (level − 1)	0	1
9	504 (level 1)	0	1
2	481 (level 0.5)	0	− 1
3	504 (level 1)	− 1	0
4	392 (level − 1)	0	0
5	481 (level 0.5)	0	0
6	504 (level 1)	1	0
7	419 (level − 0.5)	0	0

APPENDIX 3 THE POWDER X-RAY DIFFRACTION PATTERNS OF THEOPHYLLINE ANHYDROUS (FORM II, CCDC REFERENCE CODE: BAPLOT06), MONOHYDRATE (CCDC REFERENCE CODE: THEOPH01), AND COATED GRANULES WITH PRESENCE/ABSENCE OF THEOPHYLLINE MONOHYDRATE FORM

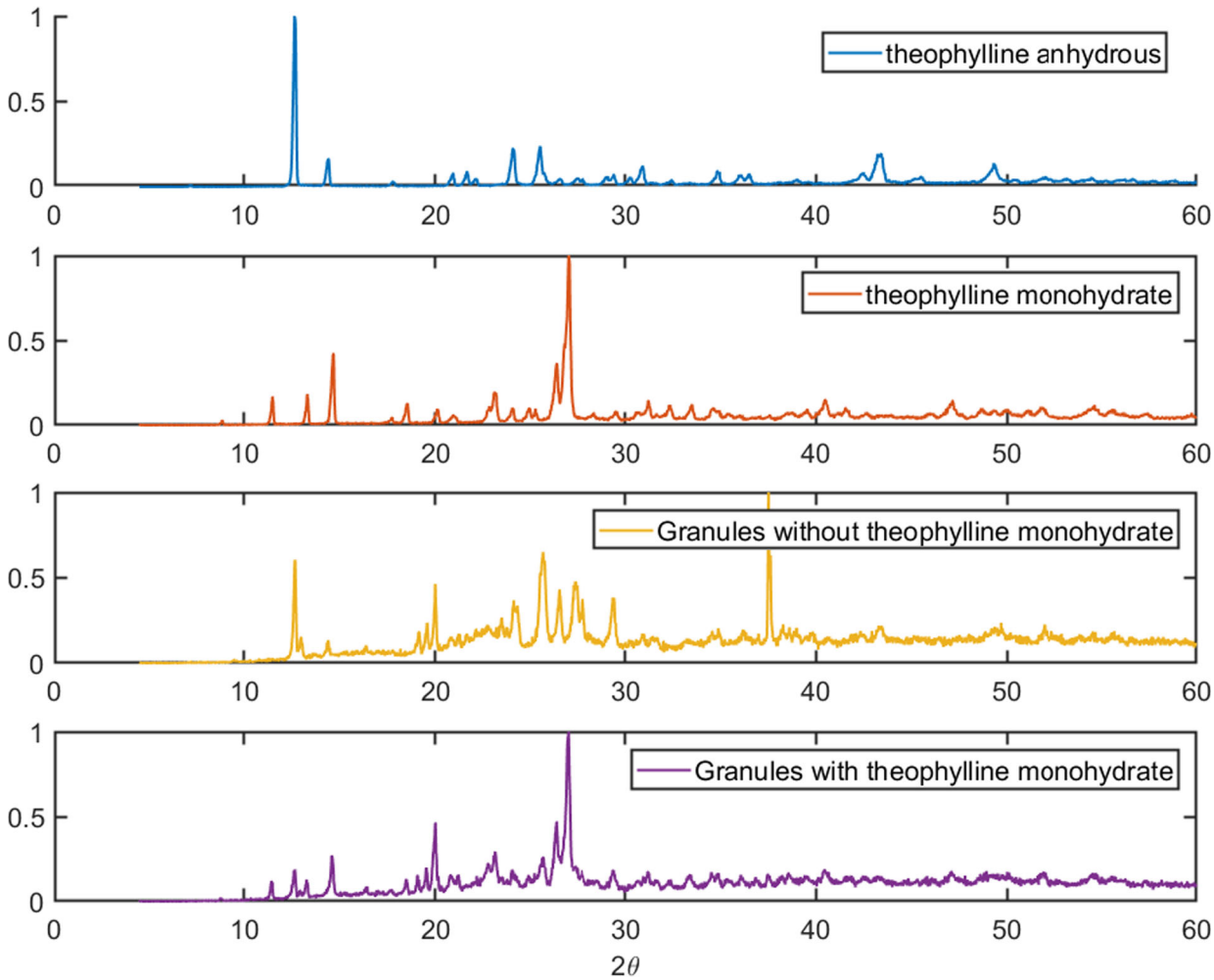

REFERENCES

1. Byrnes C, Isidori A. Output regulation for nonlinear systems: an overview. Int J Robust Nonlinear Control. 2000;10(5):323–37.
2. Corripio AB. Tuning of industrial control systems: Isa; 2000.
3. Johansson B. Feedforward control in dynamic situations. Sweden: Linköping University; 2003.
4. Yu LX. Pharmaceutical quality by design: product and process development, understanding, and control. Pharm Res. 2008;25(4):781–91.
5. Yu LX, Amidon G, Khan MA, Hoag SW, Polli J, Raju GK, *et al.* Understanding pharmaceutical quality by design. AAPS J. 2014;16(4):771–83.
6. Méndez-Acosta H, Campos-Delgado DU, Femat R, González-Alvarez V. A robust feedforward/feedback control for an anaerobic digester. Comput Chem Eng. 2005;29(7):1613–23.
7. Hattori Y, Otsuka M. Modeling of feed-forward control using the partial least squares regression method in the tablet compression process. Int J Pharm. 2017;524(1–2):407–13.
8. Westerhuis JA, Coenegracht PMJ, Lerk CF. Multivariate modelling of the tablet manufacturing process with wet granulation for tablet optimization and in-process control. Int J Pharm. 1997;156:109–17.
9. Mota J. Matrix- and reservoir- type oral multiparticulate drug delivery systems. Berlin: Freien Universität Berlin; 2010.
10. Dashevsky A, Wagner K, Kolter K, Bodmeier R. Physicochemical and release properties of pellets coated with Kollicoat SR 30 D, a new aqueous polyvinyl acetate dispersion for extended release. Int J Pharm. 2005;290(1–2):15–23.

11. Kolter K, Dashevsky A, Irfan M, Bodmeier R. Polyvinyl acetate-based film coatings. Int J Pharm. 2013;457(2):470–9.
12. The United States Pharmacopeia. Theophylline extended-release capsules. Pharm Forum. 2006;31, 185(1).
13. Carlin B, Yang S, Li JX, Felton LA. Pseudolatex dispersions for controlled drug delivery. In: Aqueous polymeric coatings for pharmaceutical dosage forms. 4th ed. Boca Raton: CRC Press; 2016. p. 11–46.
14. Farooq M, Shoaib MH, Yousuf RI, Qazi F, Hanif M. Development of extended release loxoprofen sodium multiparticulates using different hydrophobic polymers. Polym Bull. 2018:1–22.
15. Koji Muteki KY, Reid GL, Krishnan M. De-risking scale-up of a high shear wet granulation process using latent variable modeling and near-infrared spectroscopy. J Pharm Innov. 2011;6:142–56.
16. Muteki K, Swaminathan V, Sekulic SS, Reid GL. De-risking pharmaceutical tablet manufacture through process understanding, latent variable modeling, and optimization technologies. AAPS PharmSciTech. 2011;12(4):1324–34.
17. ICH Guideline. Pharmaceutical development. Q8 (2R). As revised in August. 2009.